Journal of Glaciology, Vol. 22, No. 87, 1979

SUPRAGLACIAL DEBRIS OF G2 GLACIER IN HIDDEN VALLEY, MUKUT HIMAL, NEPAL*

By M. Nakawo†

(Institute of Low Temperature Science, Hokkaido University, Sapporo, Japan 060)

Abstract. Field investigations of supraglacial debris were carried out during the monsoon season in 1974 on G2 glacier near Tukche Peak in Hidden Valley, Mukut Himal, Nepal. The thickness of the debris layer was observed to increase down-glacier. Laboratory analysis, however, showed a decrease in particle size in the same direction. This decrease is explained in terms of mixing of particles contained in glacier ice with the original debris as melting proceeds. A simple relation between debris mass and glacier flow is introduced to explain the observed results.

Résumé. *Moraines superficielles du glacier G2 de Hidden Valley, Mukut Himal, Népal.* Des recherches sur le terrain sur les moraines superficielles ont été effectuées pendant la mousson en 1974 sur le glacier G2 près de Tukche Peak de Hidden Valley, Mukut Himal, au Népal. On a observé que la couche de matériaux allait en augmentant en épaisseur d'amont à aval du glacier. Les analyses en laboratoire ont toutefois montré une diminution de la grosseur des particules dans la même direction. Cette diminution s'explique par le mélange des particules contenues dans la glace avec les débris originaux à mesure qu'elle fond. On présente une relation simple entre la masse de débris et l'écoulement du glacier afin d'expliquer les résultats observés.

Zusammenfassung. *Schutt auf der Oberfläche des G2-Gletschers im Hidden Valley, Mukut Himal, Nepal.* Während der Monsun-Periode von 1974 wurden am G2-Gletscher nahe dem Tukche Peak im Hidden Valley, Mukut Himal, Nepal, Felduntersuchungen des Oberflächenschutts durchgeführt. Die Dicke der Schuttschicht nimmt gletscherabwärts zu. Laboranalysen ergaben andererseits eine Abnahme der Partikelgrösse in derselben Richtung. Diese Abnahme wird aus der Einmischung von Partikeln aus dem Gletschereis in den ursprünglichen Schutt bei fortschreitender Abschmelzung erklärt. Eine einfache Beziehung zwischen der Schuttmasse und dem Gletscherfluss wird zur Analyse der gewonnenen Ergebnisse herangezogen.

1. Introduction

In the Nepal Himalaya, there exist a number of debris-covered glaciers of which the ablation area is mostly covered by supraglacial debris. Although a part of the debris-covered ice body near the terminus is considered to be stagnant, the other part of the ice body is still moving actively (Müller, 1968; Kodama and Mae, 1976; Nakawo and others, 1976[a]). This feature of debris-covered glaciers in the Nepal Himalaya might correspond to one of the various stages through which an active glacier passes to a fossil glacier owing to climatic change (Brown, 1925).

Many investigations of the supraglacial debris have been made in connection with the development of dirt cones (Sharp, 1949; Boulton, 1967), but only a few studies have provided particle-size distribution of the debris (Knighton, 1973). In this study, the relation between supraglacial debris and glacier flow is discussed, based on particle-size distribution data.

The field work was carried out in the monsoon season, as part of the Glaciological Expedition to Nepal, 1974, supervised by Professor K. Higuchi of Nagoya University, Nagoya, Japan (Higuchi, 1976).

2. Physical setting

Hidden Valley is located on the northern side of the Dhaulagiri Himal, the main range of the Great Himalaya, and is surrounded by several ridges with altitudes between 5 000 and 6 500 m above sea-level (Fig. 1). There are also several precipices at the outlet of the Rikha Samba Khola, the main stream in Hidden Valley. These high ridges and precipices constitute insuperable barriers to easy entry to the valley and the area is appropriately called "Hidden Valley".

* Glaciological Expedition to Nepal, Contribution No. 59.

† Present address: Geotechnical Section, Division of Building Research, National Research Council, Ottawa, Canada K1A 0R6.

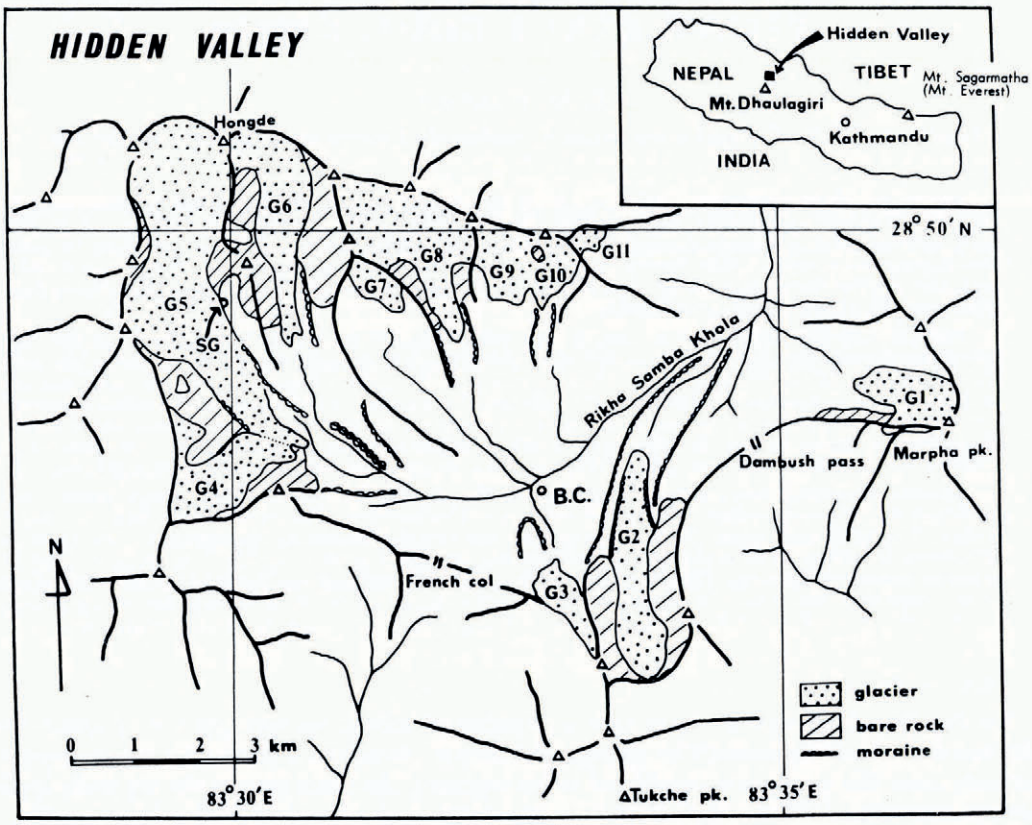

Fig. 1. Map of Hidden Valley, Mukut Himal.

The bedrock is of slate or schist in the Tibet–Tethys zone of the Paleozoic (Hagen, 1968; Hashimoto and others, 1973). The sands and gravels of the area, including the constituents of the glacial moraine, consist of flat-shaped particles of slate or schist. Most of them are red-tinged owing to lateritization processes, except for those of the recently formed glacial moraine, which are darker in colour.

At the base camp (shown as B.C. in Fig. 1, altitude 5 055 m), the mean air temperature was around 3.5°C during the monsoon season in 1974. The annual mean air temperature was estimated to be −4°C (Iwata and others, 1976) from the data obtained at Jomosom, which was the closest Nepal Government weather station. The annual precipitation at Jomosom was about 100 mm in 1974. Although the precipitation at the base camp was twice this amount, it was less than the evaporation (Shrestha and others, 1976) during the monsoon so that the area is relatively dry. The poor vegetation is a good indication of the drought condition of the area.

G2 glacier (Fig. 2) is a typical debris-covered glacier draining the northern slope of the ridge from Tukche Peak (6 915 m) to Dambush Pass (5 196 m). It is 4 km long, 0.5 km wide, and the elevation of the terminus is 5 043 m a.s.l. The firn edge has a mean elevation of about 5 350 m during the monsoon season, and an ice fall is located on the western side of the glacier at almost the same altitude, separating the debris-covered lower half from its accumulation basin. The glacier has a simple tongue shape, but is slightly curved convex to the west.

https://doi.org/10.3189/S002214300001426X Published online by Cambridge University Press

Fig. 2. G2 glacier and Tukche Peak (6 915 m).

The topographical map of the lower half of the glacier (Fig. 3), showing these features, was compiled by the stereoscopic and plane-table method (Nakawo, 1976).

Flow velocities were measured by means of marker stakes embedded in the supraglacial debris along two transverse profiles, H and I, across the glacier as shown in Figure 3 (Nakawo and others, 1976[a]). The flow velocities of 6 to 45 cm/month were obtained on profile I which was installed just below the ice fall; almost no movement was observed on profile H which was near the terminus. Nakawo (1976) explained the lack of movement in terms of the present terminus being near the 5 200 m contour line, below which the ice mass is stagnant. This is

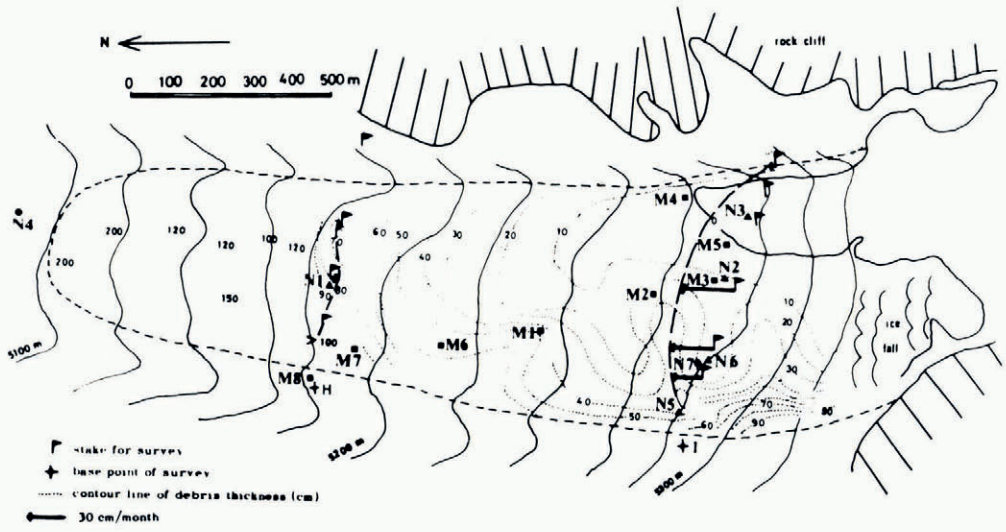

Fig. 3. Topographical map of G2 glacier. The locations marked M *are sampling locations of supraglacial debris. Melt-water samples and glacier-ice samples were obtained at the locations marked* N. *Black arrows show flow velocities. Crosses at* H *and* I *indicate surveying instrument stations. The thickness of supraglacial debris is contoured with dotted lines.*

based upon the study of air bubbles contained in glacier ice. Transverse profile of flow velocity seems to suggest that no marginal sliding takes place. If basal sliding is also assumed to be absent, the ice thickness around profile 1 can be computed to be 50 to 70 m using Nye's flow law (1952) with the estimation of an appropriate shape factor.

3. Thickness of debris layer

In Figure 3, the distribution of the debris-layer thickness of the glacier is shown by dotted lines drawn from base data of more than 100 points. A solid line adjacent to "0" indicates the boundary between debris-free ice and debris-covered ice. Measured values are shown near the terminus instead of contour lines.

The thickness of the debris layer increases progressively down-glacier from about 0 cm near the ice fall to 200 cm near the terminus. The rate of increase becomes greater down-glacier from around the contour line 5 200 m above sea-level. The debris is thicker near the margin than near the centre line of the glacier. The contours of debris-layer thickness are not symmetric with respect to the centre line of the glacier.

On the western part of the glacier there are three notable ridges of debris thickness (from west to east) that are separated by about 300 m along the glacier flow. The debris layer thickness does not increase uniformly but varies periodically; however, the general trend shows that the thickness increases down-glacier. The supraglacial debris could be considered to be nourished by rock cliffs situated on each side of the glacier since the debris layer is thicker at the margins. Debris fell from the cliffs frequently during the observation period. The largest supply of supraglacial moraine comes from the southern rock cliff near the ice fall; one of the thicker debris ridges is found at the foot of the rock cliff, but the other two ridges of thicker debris do not appear to be nourished at their present location, considering the topographical features of the glacier. It is considered, therefore, that these ridges have been nourished at the foot of the southern rock cliff near the ice fall and that two of them have been carried down to their present locations by glacier flow. If the hypothesis is correct, the periodic appearance of the ridges would indicate repeated surging and recession of the glacier or repeated degradation of the rock cliff. Since the velocity of the glacier is around 5 m/year (Nakawo and others, 1976[a]), the surging period is deduced to be about 60 years.

4. Debris samples

4.1. *Samples from supraglacial debris*

Eight samples were taken from the supraglacial debris of the glacier at locations M1 to M8 (Fig. 3) and one sample (M9) from the old lateral moraine of the glacier. Particles of gravel larger than 5 cm in diameter were discarded at the time of sampling.

Discernible differences in bulk density and water content of the samples could not be found between the samples; the *in-situ* values were 1.22 ± 0.06 Mg/m^3 and $5.5 \pm 1.0\%$ respectively. The samples M1 to M8 were composed of flat particles of slate or schist, dark in colour, while the particles in sample M9 of the old moraine were rather round and tinged with red as a result of lateritization. The difference in shape between M9 and the other samples might have had some influence on the analyses of particle-size distribution by sieving. For particles greater than 6 mm, therefore, the weight per particle was estimated; it was found to be approximately proportional to the third power of the particle size for all samples, M1 to M9. Hence, it was not necessary to take the shape difference between M9 and the others into account when the analyses of particle-size distribution were carried out.

4.2. *Samples from glacier ice and melt water*

Ice samples from the surface of the glacier were taken at locations N1, N2, N3, N5, and N6 (Fig. 3), where no debris-rich layer was found in the ice body, and melted for analyses. A

water sample at N4 was obtained from a small stream (*c.* 1 m wide and *c.* 30 cm deep) originating in the terminus of the glacier. The sample at N7 was taken from a streamlet (*c.* 20 cm wide and *c.* 10 cm deep) running on the glacier surface. The materials contained in both kinds of samples (glacier ice and melt water) were obtained by filtering each sample through filter paper. After the filter paper with the materials had been dried, the weight of the material was established.

The surface topography of the particles and their size were investigated by using a scanning electron microscope in much the same way as Kuroiwa (1970). Figure 4 shows scanning electron micrographs of the particles in the glacier ice. Similar features to those of artificially ground glacier sand taken by Kuroiwa (1970) can be seen in Figure 4A. Figure 4B shows a conchoidal fracture surface, which is one of the characteristic features of glacially derived sands (Margolis and Kennett, 1971).

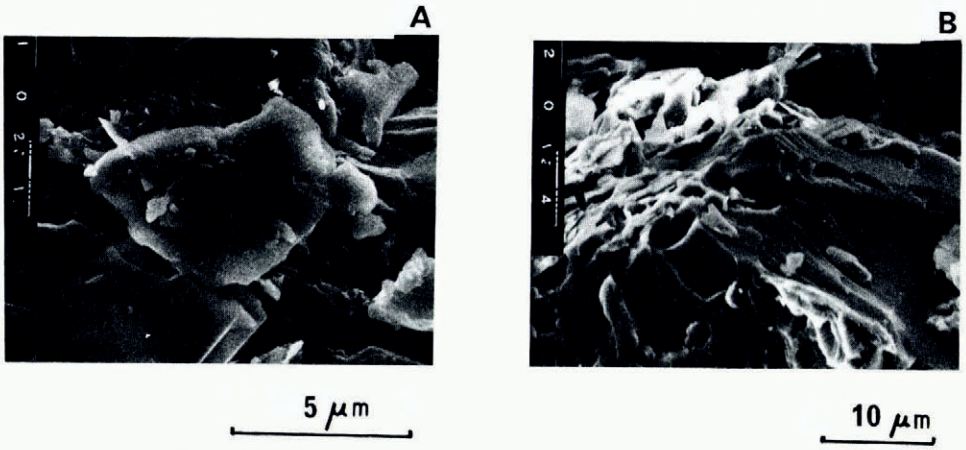

Fig. 4. Scanning electron micrographs of particles contained in glacier ice.

Observations of the debris content and particle size are tabulated in Table I. The largest debris content was found in the sample N1 from the lower glacier. The debris content of water samples N4 and N7 were rather large. The water sample values might indicate only the order of magnitude of the content, since the amount of suspended materials in flowing water varies daily and seasonally due to variations in flow velocity (Nakawo and others, 1976[b]). As for the particle size of the debris, those of N3, N5, and N6 ranged from 50 to 10 μm (5ϕ to 6ϕ) and those of N1 and N2 ranged from 500 to 50 μm (2ϕ to 5ϕ). The sizes of the particles in the water sample were small (10 to 1 μm, 6ϕ to 9ϕ) compared to the ice samples.

Table I. Content and size of particles suspended in glacier ice and melt water

Sample	*Content* mg/l	*Particle size* μm	*Remarks*
N1	865.6	100–500	Ice under debris
N2	65.6	50–200	Ice under debris
N3	221.1	10– 50	Bare ice
N4	232.2	1– 10	Run-off water
N5	10.0	10– 50	Ice under debris
N6	10.0	10– 50	Ice under debris
N7	87.8	5– 20	Running water on the glacier surface

https://doi.org/10.3189/S002214300001426X Published online by Cambridge University Press

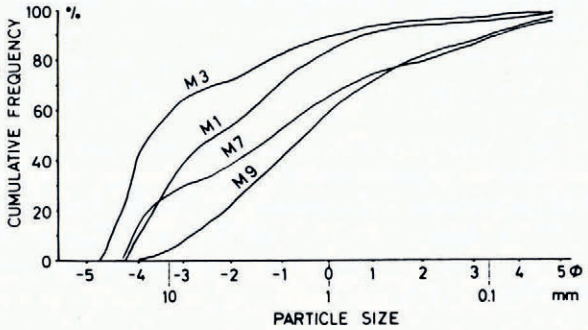

Fig. 5. Cumulative frequency curves showing the size of particles in supraglacial debris (M3, M1, and M7 from up-stream, mid-stream and down-stream in the ablation area, respectively) and old lateral moraine (M9).

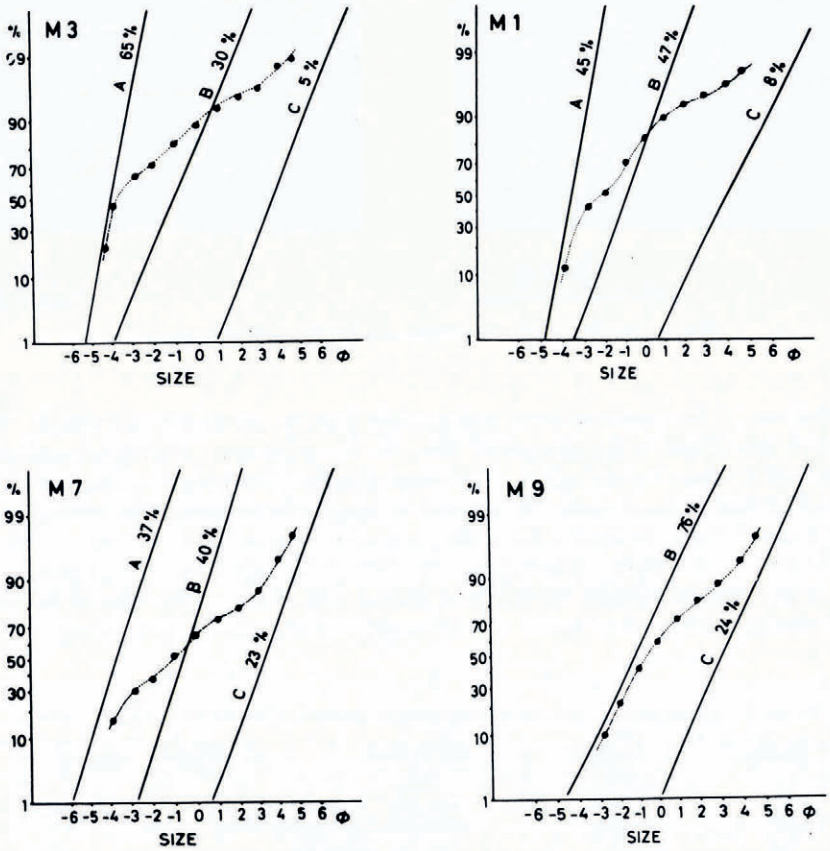

Fig. 6. Particle-size distributions of the samples plotted on log–normal probability papers. Measured values are plotted with solid circles, from which straight lines are deduced by Harding's (1949) method. The straight lines when combined give the dotted lines which are in good agreement with measured values (solid circles).

https://doi.org/10.3189/S002214300001426X Published online by Cambridge University Press

5. Analysis of particle-size distribution

Figure 5 shows the particle-size cumulative frequency distributions obtained by sieving through several screens with an interval of about 1ϕ. The particles become progressively finer down-glacier (from M3 to M7); the particles from the old lateral moraine M9 were the finest. The particle-size distributions of the samples are plotted as solid circles on log–normal probability paper in Figure 6. These plotted points do not lie on a straight line, i.e. the distribution is not a normal distribution.

Harding (1949) developed a graphical method by which he could separate a certain polymodal distribution into several normal distributions. By applying this method, it was found that the particle-size distribution of each sample could be represented by two or three unequal and overlapping linear populations, as shown by the straight lines on the graphs in Figure 6, e.g. the mixing of normal distributions A, B, and C with weights of 65, 30, and 5% gives the dotted curve in M3 (Fig. 6). The resulting composite curve agrees well with the measured values as shown in the figure. Hence, the particle-size distribution of each sample can be completely expressed by two or three normal distributions each of which is defined by its mean and standard deviation and its relative proportion by weight. The results of this analysis for each sample are tabulated in Table II. The median particle size and quartile-deviation of the original (observed) distributions are also tabulated in the same table.

Table II. Results of particle-size distribution analyses of supraglacial debris and old lateral moraine

			M1	M2	M3	M4	M5	M6	M7	M8	M9
Median diameter		mm	4.59	3.61	12.55	12.13	8.88	2.73	2.14	2.07	1.41
Quartile deviation		mm	5.04	5.12	7.62	6.28	5.60	3.76	4.54	4.75	1.60
A	dm*	ϕ	−3.6	−3.6	−4.0	−4.0	−3.6	−3.4	−3.7	−3.8	
	σ_0	ϕ	0.5	0.6	0.6	0.6	0.4	0.6	1.0	0.55	
	w	%	45	44	65	70	60	36	37	33	
B	dm	ϕ	−0.9	−0.85	−1.05	−1.2	−1.15	−1.0	−0.6	−0.8	−1.2
	σ_0	ϕ	1.1	0.9	1.25	1.0	0.9	0.9	0.95	1.0	1.5
	w	%	47	47	30	26	35	40	40	40	76
C	dm	ϕ	+4.0	+3.25	+3.7	+2.65	+2.15	+2.7	+3.3	+3.4	+3.15
	σ_0	ϕ	1.5	1.65	1.25	2.7	1.5	1.25	1.2	1.3	1.35
	w	%	8	9	5	4	5	24	23	27	24

* dm, σ_0, and w are median diameter, standard deviation, and mixing ratio, respectively.

As shown in Table II, the size distributions of all samples from the supraglacial debris (M1 to M8) are the mixture of three normal distributions A, B, and C, while that of M9 consists of two distributions. Similar values of −3.4 to −4.0 and about 0.5 in ϕ scale are obtained for the mean and the standard deviation respectively of the normal distributions designated A for each of the samples. The mean and the standard deviation of the normal distributions designated B have the values of −0.6 to −1.2 and about 1.0 in ϕ scale respectively, and those designated C have the values of +2.1 to +4.0 and about 1.5 in the ϕ scale. Hence a normal distribution designated by A, B, or C for each sample is considered to belong to the unique population A, B, or C respectively (Inokuchi and Mezaki, 1974[a], [b]). The difference in the percentage content by weight (or mixing ratios) of the populations A, B, and C is, therefore, the main reason for the difference between the observed distributions.

The mixing ratios of A (coarse), B (middle), and C (fine) of the samples M3, M4, and M5 taken up-stream are more than 60%, about 30%, and less than 5% respectively. The relative concentration of A (coarse) decreases down-glacier from more than 60% for the upper region, to about 45% at middle (M1 and M2) and about 35% for the lower region (M6, M7, and M8). The relative concentration of C (fine) increases down-glacier from less than 5% for the upper samples, to about 9% for the middle samples, and to around 25% for the lower samples. A

discernible change was not observed in the relative concentration of B. For the sample M9 of the old lateral moraine, the relative concentration for C has a value similar to that of the lower sample.

6. Discussion

6.1. *Decrease in particle size down-glacier*

The pairs of quartile deviation and median diameter of particle-size distributions are often plotted on log–log paper to determine whether their graphic distributions are distinctive, and to examine the sedimentological implications. A group of distributions lying between two lines of slope of less than 45° (i.e. in the area between two broken lines in Fig. 7) was found among a number of particle-size distributions of several kinds of sediments taken from various glaciers (Buller and McManus, 1973). They considered the low-slope distribution to be caused by the addition of a finer population to a coarser population.

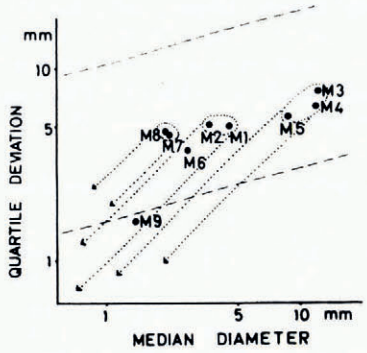

Fig. 7. Relationship of quartile deviation to median diameter, showing a trend of low gradient (the area between broken lines is after Buller and McManus, 1973). Dotted arrows correspond to weathering process.

The quartile-deviation versus median-diameter relationship of each sample taken from the G2 glacier is also shown in Figure 7. The results for samples M1 to M8 all lie in the region defined by Buller and McManus (1973) and define the same general slope. This agreement suggests that the addition of finer particles causes the change in population characteristics in the direction of the flow.

The relative proportion of fine particles increases down-glacier since the average particle size decreases down-glacier. The observations indicate that population C, in which the mixing ratio increases down-glacier as shown in Table II, caused the change in the population characteristics.

The particles contained in the glacier ice are from 2ϕ to 6ϕ in size, while those in the melt water are from 6ϕ to 9ϕ (Table I). Since the range of the particle-size of population C is from 2ϕ to 6ϕ (Fig. 6, Table II), the particles in the glacier ice could be from population C. It is feasible, therefore, that the finer particles contained in the glacier ice are added to the glacier surface and mixed with the original debris during melting, resulting in the down-glacier decrease in the average particle size.

6.2. *Relation to glacier flow*

When each debris sample was taken, about half the mass, which consisted of particles greater than 5 cm, was discarded. The mass of population C per unit area of glacier surface, m_c, therefore, can be approximately expressed as:

$$m_c = \tfrac{1}{2} d \rho w_c, \qquad (1)$$

https://doi.org/10.3189/S002214300001426X Published online by Cambridge University Press

where d and ρ are the depth and the bulk density of the supraglacial debris respectively, and w_c is the mixing ratio of the finer particles of population C.

In Figure 8, d and w_c are shown by a solid line and solid circles respectively, along an estimated flow line near the centre of the glacier. The debris thickness is simplified to the dashed line in the figure because the peak in the debris thickness is due to the enormous supply at the foot of the ice fall as mentioned in Section 3. The mixing ratio w_c is also assumed to a first approximation, and is represented by the dotted line in Figure 8. With these assumptions, m_c can be determined as a function of position using Equation (1), since ρ is considered to be constant as mentioned in Section 4.

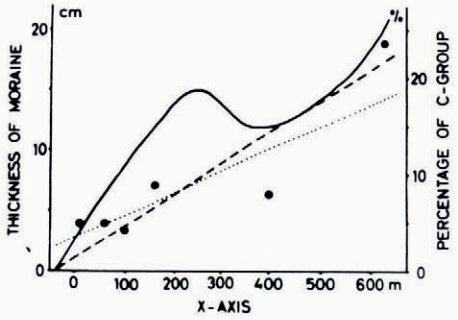

Fig. 8. Thickness of debris and mixing ratio of population C along a flow line. Solid line is debris thickness, which is simplified to the dashed line. Mixing ratio of population C is assumed to be dotted line from the base data of solid circles.

The morphology of G2 glacier is so simple (Fig. 3) that the flow lines can be considered to be parallel. Assume the x-axis to be positive down-glacier. Then the continuity equation of debris mass of population C, m_c, is

$$\frac{\partial m_c}{\partial t}+\frac{\partial}{\partial x}(vm_c) = s_c, \tag{2}$$

where t and v are time and surface flow velocity respectively, and s_c is the rate of debris supply to the supraglacial debris. Since the finer debris particles (population C) are considered to be supplied by the melting ice as discussed in the previous section, s_c can be written as

$$s_c = ac, \tag{3}$$

where a and c are the ablation rate of ice under debris and the debris content in ice respectively. Combining Equations (2) and (3) with the assumption of steady state of the glacier, gives

$$\frac{\mathrm{d}}{\mathrm{d}x}(vm_c) = ac. \tag{4}$$

It is said that the supraglacial debris controls the ablation rate of glacier ice under it; namely, the ablation rate is accelerated under a thin debris layer and is retarded under a thick one as compared with that of bare ice surfaces (Loomis, 1970; Moribayashi and Higuchi, 1972; Small and Clark, 1974). In Nepal Himalaya, Fujii (1977) conducted an experiment on the ablation rate control by a debris layer up to 8 cm in thickness on a snow patch adjacent to Rikha Samba Glacier, which is located also in Hidden Valley, Mukut Himal, and obtained similar results.

Unfortunately, the ablation rate of the G2 glacier surface was not measured and was therefore estimated as follows. The ablation rate measured on the bare ice surface of Rikha Samba Glacier (Fujii and others, 1976) was corrected by the use of Fujii's relation for the

https://doi.org/10.3189/S002214300001426X Published online by Cambridge University Press

range below 8 cm in debris thickness. In the area of G2 glacier where the debris thickness is greater than 8 cm, the ablation rate was estimated to be one third of the bare-ice value obtained at Rikha Samba Glacier by extrapolation of Fujii's results, since no data have been obtained concerning the ablation of ice under debris layers of thickness greater than about a few tens of centimetres. The ablation rate a in Equation (4), is thus obtained as a function of position x.

For simplification, the debris content in the ice, c, was assumed to be constant and to have an average of the measured values in Table I, since debris-rich layers were rarely seen. The surface velocity v was estimated as a function of position x by substituting m_c, a, and c in Equation (4). A flow velocity of about 10 m/year was calculated for a location where a flow velocity of about 5 m/year was actually measured (Nakawo and others, 1976[a]). The assumption of steady flow may result in a larger value of the estimated flow velocity than the measured one.

This good agreement, however, is in itself not particularly significant, considering the assumptions and many simplifications. Nevertheless, the calculations indicate that the observed amount of supraglacial debris resulting from melting ice is about what would be expected from the measurements of the flow velocity. This simple relation between the supraglacial debris distribution and glacier flow (Equations (1), (2), (3), and (4)), therefore, could be introduced into models of the dynamic response of debris-covered glaciers (e.g. response to climatic change) with the reservation that adjustments would have to be made from more detailed observations and experiments.

Acknowledgements

The author would like to express his gratitude to the members of the Glaciological Expedition to Nepal, 1974, to His Majesty's Government of Nepal and to many Himalayan people for helping him and enabling him to carry out the investigation. The author is indebted to Professor G. Wakahama of Hokkaido University, Sapporo, Japan, for helping him to join the Expedition and giving him many valuable suggestions. Thanks are due to Dr Y. Suzuki and Mr H. Taishi of Hokkaido University for many helpful discussions.

MS. received 11 July 1978

REFERENCES

Boulton, G. S. 1967. The development of a complex supraglacial moraine at the margin of Sørbreen, Ny Friesland, Vestspitsbergen. *Journal of Glaciology*, Vol. 6, No. 47, p. 717–35.

Brown, W. H. 1925. A probable fossil glacier. *Journal of Geology*, Vol. 33, No. 4, p. 464–66.

Buller, A. T., *and* McManus, J. 1973. The quartile-deviation/median-diameter relationships of glacial deposits. *Sedimentary Geology*, Vol. 10, No. 2, p. 135–46.

Fujii, Y. 1977. Field experiment on glacier ablation under a layer of debris cover. *Seppyō*, Vol. 39, Special Issue, p. 20–21.

Fujii, Y., *and others*. 1976. Mass balance studies of the glaciers in Hidden Valley, Mukut Himal, [by] Y. Fujii, M. Nakawo [i.e. Nakao], and M. L. Shrestha. *Seppyō*, Vol. 38, Special Issue, p. 17–21.

Hagen, T. 1968. Report on the geological survey of Nepal. Vol. 2: geology of the Thakkhola including adjacent areas. *Denkschriften der Schweizerischen Naturforschenden Gesellschaft*, Bd. 86/2.

Harding, J. P. 1949. The use of probability paper for the graphical analysis of polymodal frequency distributions. *Journal of the Marine Biological Association*, Vol. 28, No. 1, p. 141–53.

Hashimoto, S., *and others*. 1973. *Geology of Nepal Himalayas, by S. Hashimoto, Y. Ohta, and C. Akibe*. Tokyo, Saikon Publishing Co. Ltd.

Higuchi, K. 1976. Outline of the glaciological expedition to Nepal. *Seppyō*, Vol. 38, Special Issue, p. 1–5.

Inokuchi, M., *and* Mezaki, S. 1974[a]. Chūsekikasen ni okeru kashō sareki no ryūdo sosei ni tsuite (I) [Study on the grain size distribution of bed materials in alluvial rivers (I)]. *Tōkyō Kyōiku Daigaku Chiri-gaku Kenkyū Hōkoku: Tokyo Geography Papers*, No. 18, p. 25–38.

Inokuchi, M., *and* Mezaki, S. 1974[b]. Chūsekikasen ni okeru kashō sareki no ryūdo sosei ni tsuite (II) [Analysis of the grain size distribution of bed materials in alluvial rivers (II)]. *Chiri-gaku Hyōron: Geographical Review of Japan*, Vol. 47, No. 9, p. 545–55.

Iwata, S., *and others*. 1976. Nepal Himalaya no kōzōdo [Patterned ground in the Nepal Himalaya]. [By] S. Iwata, Y. Fujii, K. Higuchi. *Chigaku Zasshi: Journal of Geography*, Vol. 85, No. 3, p. 21–39.

Knighton, A. D. 1973. Grain-size characteristics of supraglacial dirt. *Journal of Glaciology*, Vol. 12, No. 66, p. 522–24. [Letter.]

Kodama, H., *and* Mae, S. 1976. The flow of glaciers in the Khumbu region. *Seppyō*, Vol. 38, Special Issue, p. 31–36.

Kuroiwa, D. 1970. Noruwee no Nigardsbreen yori hōshutsu sareta hyōgasa to shiruto no hyōmen-kōzō to kōbutsu-seibun ni tsuite [Surface topography and mineral compositions of silt and sand discharged from Nigardsbreen in Norway]. *Teion-kagaku: Low Temperature Science*, Ser. A, [No.] 28, p. 97–104.

Loomis, S. R. 1970. Morphology and ablation processes on glacier ice. *Proceedings of the Association of American Geographers*, Vol. 2, 1970, p. 88–92.

Margolis, S. V., *and* Kennett, J. P. 1971. Cenozoic paleoglacial history of Antarctica recorded in subantarctic deep-sea cores. *American Journal of Science*, Vol. 271, No. 1, p. 1–36.

Moribayashi, S., *and* Higuchi, K. 1972. Yūsetsu no jinkō yokusei ni kansaru kisoteki kenkyū [On experiments on reducing the melting of snow]. *Seppyō*, Vol. 34, No. 4, p. 165–72.

Müller, F. 1968. Mittelfristige Schwankungen der Oberflächengeschwindigkeit des Khumbugletschers am Mount Everest [Medium-term fluctuations of the surface movement of the Khumbu glacier, Mount Everest region]. *Schweizerische Bauzeitung*, Jahrg. 86, Ht. 31, p. 569–74.

Nakawo [i.e. Nakao], M. 1976. Bubble pattern of a glacier near Tukche Peak in Hidden Valley, Mukut Himal. *Seppyō*, Vol. 38, Special Issue, p. 44–49.

Nakawo [i.e. Nakao], M., *and others*. 1976[a]. Flow of glaciers in Hidden Valley, Mukut Himal, [by] M. Nakawo [i.e. Nakao], Y. Fujii, and M. L. Shrestha. *Seppyō*, Vol. 38, Special Issue, p. 39–43.

Nakawo [i.e. Nakao], M., *and others*. 1976[b]. Water discharge of Rikha Samba Khola in Hidden Valley, Mukut Himal, [by] M. Nakawo [i.e. Nakao], Y. Fujii, and M. L. Shrestha. *Seppyō*, Vol. 38, Special Issue, p. 27–30.

Nye, J. F. 1952. The mechanics of glacier flow. *Journal of Glaciology*, Vol. 2, No. 12, p. 82–93.

Sharp, R. P. 1949. Studies of superglacial debris on valley glaciers. *American Journal of Science*, Vol. 247, No. 5, p. 289–315.

Shrestha, M. L., *and others*. 1976. Climate of Hidden Valley, Mukut Himal during the monsoon in 1974, [by] M. L. Shrestha, Y. Fujii, and M. Nakawo [i.e. Nakao]. *Seppyō*, Vol. 38, Special Issue, p. 105–08.

Small, R. J., *and* Clark, M. J. 1974. The medial moraines of the lower Glacier de Tsidjiore Nouve, Valais, Switzerland. *Journal of Glaciology*, Vol. 13, No. 68, p. 255–63.